
–Appendix–

Dynamically Masked Discriminator for GANs

Anonymous Author(s)

Affiliation

Address

email

Abstract

1 In this supplementary material, we first introduce the implementation details of
2 our Dynamic Mask Discriminator (DMD), and then provide more technical de-
3 tails of the proposed DMD in Sec. 1. In Sec. 2.1, we elaborate on the additional
4 details of datasets and experiment settings. In Sec. 2.3, we provide additional
5 experimental results, where our DMD is integrated with more GANs models
6 We also report the error bars of our method in Sec. 3 and describe the broader
7 impact (Sec. 4) and limitation (Sec. 5) of our method.

8 1 Implementation Details

9 In this section, we provide the implementation details of our proposed method. We have utilized the
10 PyTorch [15] public platform to conduct our experiments. Our models were trained on a workstation
11 equipped with 8 NVIDIA Tesla V100 GPUs with 32 GB memory capacity, a CPU of 2.8GHz, and
12 512GB RAM.

13 1.1 More details of the proposed method.

14 Our method is designed to automatically detect the retardation of the discriminator and force it to
15 fast learn the new knowledge given time-varying distributions of generated samples. To show the
16 detailed strategy of the proposed DMD method, the pseudo-code is given in Algorithm. 1. In our
17 main paper, we have demonstrated the effectiveness of our proposed DMD method by integrating it
18 with image generation techniques on StyleGAN-V2 [9].

19 Since the retardation of learning new knowledge can potentially be addressed by augmenting the
20 input stream or the outcome of the discriminator, we also extend another two schemes to achieve
21 dynamic discriminator adjustment. Besides the proposed dynamic feature masking scheme, we can
22 dynamically mask the input and output of the discriminator when it is detected as retardation. The
23 corresponding details are shown summarized in Algorithm. 2 and Algorithm. 3.

24 1.2 More details of model parameter difference

25 We detail *model parameter difference* which is used in the main paper Figure 3(a) for investigating
26 the fixed discriminator of StyleGAN-V2. Model parameter difference metric is to measure the
27 differences of the discriminator model weights between two adjacent training steps:

$$\mathbf{d}_{t_j} = \|W_{t_j}^d - W_{t_{j-1}}^d\|^2 \quad (1)$$

28 where $W_{t_j}^d$ is the parameter weight of d -th layer of the discriminator during t_j training step, and
29 $\|\cdot\|^2$ is L2 norm. A smaller \mathbf{d}_{t_j} indicates that the parameter weights of d -th layer at t_j training step

30 are more similar to that at (t_{j-1}) training step, *i.e.*, parameter weights are updated slowly. In other
 31 words, given new arrival generated samples with new distributions, a smaller \mathbf{d}_{t_j} indicates that the
 32 discriminator slows down the learning of new knowledge to some extent. In the main paper, we
 33 calculate \mathbf{d}_i in the full connection layer of the discriminator.

Algorithm 1 Dynamic Mask Discriminator

Require:

Generator \mathcal{G}_{θ^t} ; Current Discriminator $D_\phi(\cdot)$; Non-Masked Discriminator $\mathcal{D}_\phi(\cdot)$; Dynamically
 Masked Discriminator $\bar{D}_\phi(\cdot)$; Training Step t ;
 d -th Layer of Discriminator $\mathbf{F}^{(d),t}$; Dynamic Mask \mathbf{m}_d^t ;
 d -th Masking Layer of Discriminator $\bar{\mathbf{F}}^{(d),t}$; Predefined Threshold λ ; Retardation Metric R_t ;
 Set U_t Containing m Samples for Calculating Retardation Metric;
 The number of training steps n_t ; The number of images per training step n_s ;

Ensure:

Initialize $R_t \leftarrow 0$ and $t \leftarrow 1$; Random \mathbf{m}_d^t ;
 1: **while** θ has not converged **do**
 2: **for** $t = 1$ to n_t **do**
 3: **if** $R_t > \lambda$ **then**
 4: $\mathbf{M}^t \leftarrow \mathbf{m}_d^t$; $\mathbf{M}_T \leftarrow \mathbf{M}^t$; $D_\phi(\cdot) \leftarrow \bar{D}_\phi(\cdot)$
 5: **else**
 6: $\mathbf{M}^t \leftarrow \text{vector}(1)$; $\mathbf{M}_T \leftarrow \mathbf{m}_d^{t+1}$; $D_\phi(\cdot) \leftarrow \mathcal{D}_\phi(\cdot)$
 7: **end if**
 8: **for** $s = 1$ to n_s **do**
 9: $\bar{\mathbf{F}}^{(d),t} \leftarrow \mathbf{F}^{(d),t} \odot \mathbf{M}^t$
 10: $L_{\phi(t)} \leftarrow -\mathbb{E}_{I,t}[\log(D_\phi(I))] - \mathbb{E}_{z \sim p_{z,t}}[\log(1 - D_\phi(\mathcal{G}(z, \theta^t)))]$
 11: $\theta_s \leftarrow \text{Adam}(\frac{\partial \phi(t)}{\partial \theta_{s-1}})$;
 12: **end for**
 13: $\mathcal{R}_t = \frac{1}{m} \sum_{i \in U_t} \frac{\bar{\mathbf{F}}_i^{(d),t} \cdot \mathbf{F}_i^{(d),t}}{|\bar{\mathbf{F}}_i^{(d),t}| |\mathbf{F}_i^{(d),t}|}$
 14: **end for**
 15: **end while**
 16: **Return** θ ;

34 2 Additional Details on Experiments

35 2.1 Datasets and Experimental Settings

36 **AFHQ-V2** [2] consists of 3 independent sub-datasets, which include around 5,000 closeups of cat,
 37 dog, and wildlife faces, respectively (denoted as **AFHQ-Cat**, **AFHQ-Dog**, and **AFHQ-Wild**). We
 38 utilized a high-quality Lanczos filter [11] to resize all images to a resolution of 256×256 . We
 39 then conducted experiments on three sub-datasets while setting StyleGAN-V2 [9] as the baseline
 40 model. We maintain consistency with ADA [6], by using identical network architectures [9], weight
 41 demodulation [9], style mixing regularization [8], path length regularization, lazy regularization
 42 [9], equalized learning rate for all trainable parameters [5], non-saturating logistic loss [3] with R_1
 43 regularization [14], and the Adam optimizer [10].

44 **FFHQ** [8] comprises 70,000 images of human faces, which we used for training after downscaling
 45 them to a resolution of 256×256 . In this case, we set StyleGAN-V2 [9] as the baseline and used
 46 the same settings as those for AFHQ-V2.

47 **LSUN-Church** [19] includes 126,000 images of outdoor church. We downscale them to 256×256
 48 as the training data. In this case, we also set StyleGAN-V2 [9] as the baseline and used the same
 49 settings as those for FFHQ.

50 2.2 Baselines

51 In accordance with previous studies [6, 4, 13], we have integrated our proposed method with
 52 StyleGAN-V2 [9]. In order to assess the effectiveness of our method, we have compared it with

Algorithm 2 Dynamic Mask Discriminator Assert in Input (*Input Masking*)

Require:

Generator \mathcal{G}_{θ^t} ; Discriminator $\mathcal{D}_{\phi}(\cdot)$; Training Step t ; Dynamic Mask \mathbf{m}^t ;
 Predefined Threshold λ ; Retardation Metric R_t ;
 Set U_t Containing m Samples for Calculating Retardation Metric;
 d -th Layer of Discriminator $\mathbf{F}^{(d),t}$; After Masking Input $\tilde{\mathbf{F}}^{(d),t}$;
 The number of training steps n_t ; The number of images per training step n_s ;

Ensure:

Initialize $R_t \leftarrow 0$ and $t \leftarrow 1$; Random \mathbf{m}^t ;
 1: **while** θ has not converged **do**
 2: **for** $t = 1$ to n_t **do**
 3: **if** $R_t > \lambda$ **then**
 4: $\mathbf{M}^t \leftarrow \mathbf{m}^t$; $\mathbf{M}_T \leftarrow \mathbf{M}^t$;
 5: **else**
 6: $\mathbf{M}^t \leftarrow \text{vector}(1)$; $\mathbf{M}_T \leftarrow \mathbf{m}^{t+1}$;
 7: **end if**
 8: **for** $s = 1$ to n_s **do**
 9: $\tilde{\mathbf{I}} \leftarrow \mathbf{I} \odot \mathbf{M}^t$; $\tilde{\mathbf{I}} \leftarrow \mathcal{G}(z, \theta^t) \odot \mathbf{M}^t$
 10: $L_{\phi(t)} \leftarrow -\mathbb{E}_{\tilde{\mathbf{I}}, t}[\log(D(\tilde{\mathbf{I}}))] - \mathbb{E}_{z \sim p_{z,t}}[\log(1 - D(\tilde{\mathbf{I}}))]$
 11: $\theta_s \leftarrow \text{Adam}(\frac{\partial \phi(t)}{\partial \theta_{s-1}})$;
 12: **end for**
 13: $\mathcal{R}_t = \frac{1}{m} \sum_{i \in U_t} \frac{\tilde{\mathbf{F}}_i^{(d),t} \cdot \mathbf{F}_i^{(d),t}}{|\tilde{\mathbf{F}}_i^{(d),t}| |\mathbf{F}_i^{(d),t}|}$
 14: **end for**
 15: **end while**
 16: **Return** θ ;

53 state-of-the-art methods that improve discriminators through data augmentation, including ADA [6]
 54 and APA [4]. We have also compared our method with GANs that utilize regularization techniques,
 55 such as LC-Reg [16], zCR [20], InsGen [18], Adaptive Dropout [6], AdaptiveMix [13], MEE [12],
 56 and DynamicD [17].

57 2.3 Additional Experimental Results

58 **Combining our method with more GAN models.** To further show the effectiveness of our method,
 59 we additionally replace the discriminator of StyleGAN-V3 [7] with the proposed DMD, where
 60 StyleGAN-V3 contains two versions *i.e.*, StyleGAN-V3T and StyleGAN-V3R. Table A1 shows our
 61 method improves the FID of StyleGAN-V3R from 7.616 to 6.864, and improves that of StyleGAN-
 62 V3T from 5.850 to 4.921. This is because our method facilitates the training of StyleGAN-V3’s
 63 generator.

Table A1: Our method over StyleGAN-V3 [7] on AFHQ-Cat.

| | FID ↓ | IS ↑ |
|---------------------------|--------------|--------------|
| StyleGAN-V3R | 7.616 | 1.881 |
| StyleGAN-V3R w/ Ours(DMD) | 6.864 | 1.915 |
| StyleGAN-V3T | 5.850 | 1.916 |
| StyleGAN-V3T w/ Ours(DMD) | 4.921 | 1.969 |

64 **Additional Generated Distribution** Our main paper studies the generated distributions of
 65 StyleGAN-V2. Here, we additionally provide the distribution of the generated samples of APA
 66 [4] method on FFHQ[8] in Fig. A1. Fig. A1 also indicates that the generated distributions undergo
 67 dynamical and complex changes over time as the generator evolves during training. As a result,
 68 the generated samples are not independently and identically distributed (i.i.d) across the training
 69 progress, posing significant challenges in learning the generated distributions.

Algorithm 3 Dynamic Mask Discriminator Assert in Outcome Logits (*Dynamic Head*)

Require:

- Generator \mathcal{G}_{θ^t} ; Discriminator $\mathcal{D}_{\phi}(\cdot)$; Training Step t ;
- Outcome Logit Number of $\mathcal{D}_{\phi}(\cdot)$ and $\bar{\mathcal{D}}_{\phi}(\cdot)$ k ; Dynamic Mask \mathbf{m}^t ;
- d -th Layer of Discriminator $\mathbf{F}^{(d),t}$; After Masking Outcome Logits $\bar{\mathbf{F}}^{(d),t}$;
- Predefined Threshold λ ; Retardation Metric R_t ;
- Set U_t Containing m Samples for Calculating Retardation Metric;
- The number of training steps n_t ; The number of images per training step n_s ;

Ensure:

- Initialize $R_t \leftarrow 0$ and $t \leftarrow 1$; Random \mathbf{m}^t ;
 - 1: **while** θ has not converged **do**
 - 2: **for** $t = 1$ to n_t **do**
 - 3: **if** $R_t > \lambda$ **then**
 - 4: $\mathbf{M}^t \leftarrow \mathbf{m}^t$; $\mathbf{M}_T \leftarrow \mathbf{M}^t$;
 - 5: **else**
 - 6: $\mathbf{M}^t \leftarrow \text{vector}(1)$; $\mathbf{M}_T \leftarrow \mathbf{m}^{t+1}$;
 - 7: **end if**
 - 8: **for** $s = 1$ to n_s **do**
 - 9: $L_{\phi(t)} \leftarrow -\mathbb{E}_{I,t}[\log(\sum(D(I) \odot \mathbf{M}^t))] - \mathbb{E}_{z \sim p_{z,t}}[\log(1 - \sum(D(\mathcal{G}(z, \theta^t)) \odot \mathbf{M}^t))]$
 - 10: $\theta_s \leftarrow \text{Adam}(\frac{\partial \phi(t)}{\partial \theta_{s-1}})$;
 - 11: **end for**
 - 12: $\mathcal{R}_t = \frac{1}{m} \sum_{i \in U_t} \frac{\bar{\mathbf{F}}_i^{(d),t} \cdot \mathbf{F}_i^{(d),t}}{|\bar{\mathbf{F}}_i^{(d),t}| |\mathbf{F}_i^{(d),t}|}$
 - 13: **end for**
 - 14: **end while**
 - 15: **Return** θ ;
-

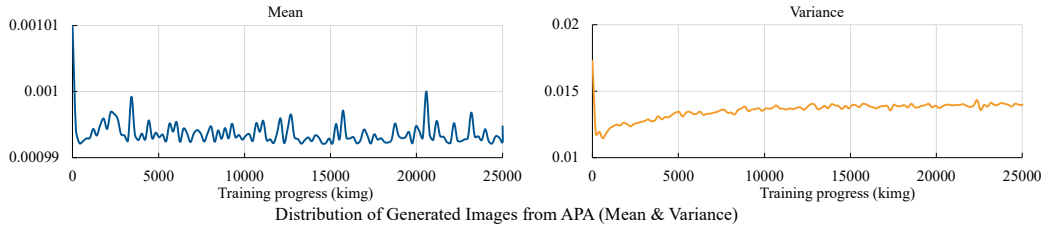


Figure A1: Illustration of time-varying distributions of generated samples in the training process of APA [4] on FFHQ [8]. The mean and variance generated samples' features show the generated distributions are dynamic and time-varying during training, as the generator evolves.

70 3 Error Bar

71 To evaluate the reproducibility of our method's results, we run our experiments three times using
72 random seeds and the same hyper-parameters. Table A2 and Table A3 list the mean and variance of
73 experimental results to show the error bar.

74 As shown in Table A2 and Table A3, our method performs stably on multiple datasets *i.e.*, AFHQ-
75 V2, FFHQ and LSUN-Church datasets, indicating the reproducibility of our method.

76 4 Broader Impact

77 In this paper, we propose a novel method to improve the training of GANs, helping to generate
78 high-quality images. Our method can be used for various applications such as producing training
79 data and creating photorealistic images. On the other hand, like other generative models, our method
80 can be misused for the application of Deepfake [1], where fake content is synthesized to deceive and
81 mislead people, leading to a negative social impact. Nevertheless, many researchers have considered
82 this problem, while exploring fake content detection and media forensics techniques. In addition, we

Table A2: Quantitative results of our method on AFHQ-V2 dataset [2], error bars are reported in terms of mean and variance, and Ours is StyleGAN-V2+DMD

| | AFHQ-Cat | | AFHQ-Dog | | AFHQ-Wild | |
|------------------------------|-------------|-------------|--------------|-------------|-------------|-------------|
| | FID ↓ | IS ↑ | FID ↓ | IS ↑ | FID ↓ | IS ↑ |
| StyleGAN-V2 | 7.924 | 1.890 | 26.310 | 9.000 | 3.957 | 5.567 |
| Ours (Reported in the paper) | 5.879 | 1.988 | 21.240 | 9.698 | 3.471 | 5.647 |
| Ours (re-run-1)) | 5.896 | 1.944 | 20.016 | 9.807 | 3.473 | 5.803 |
| Ours (re-run-2)) | 6.015 | 1.987 | 20.456 | 10.291 | 3.420 | 5.699 |
| Ours(Mean±Variance) | 5.930±0.061 | 1.973±0.021 | 20.571±0.506 | 9.932±0.258 | 3.455±0.025 | 5.716±0.065 |

Table A3: Quantitative results of our method on FFHQ [8] and LSUN-Church [19], where error bars are reported in terms of mean and variance, and Ours is StyleGAN-V2+DMD.

| | LSUN-Church (126K) | | FFHQ(70K) | |
|------------------------------|--------------------|-------------|-------------|-------------|
| | FID ↓ | IS ↑ | FID ↓ | IS ↑ |
| StyleGAN-V2 | 4.292 | 2.589 | 3.810 | 5.185 |
| Ours (Reported in the paper) | 3.061 | 2.792 | 3.299 | 5.204 |
| Ours (re-run-1)) | 3.025 | 2.795 | 3.177 | 5.225 |
| Ours (re-run-2)) | 2.993 | 2.787 | 3.285 | 5.200 |
| Ours(Mean±Variance) | 3.026±0.028 | 2.791±0.003 | 3.254±0.055 | 5.210±0.011 |

83 believe there would be regulations on fake content generation, such as forcing synthesized content
 84 to be injected with identifications that indicate it to be fake.

85 5 Limitations

86 By observing the time-varying distributions of the samples generated by the generator, we inno-
 87 vatively propose a method for training GANs, from the perspective of online continual learning.
 88 In this paper, we mainly show the challenges posed by the time-varying distributions, reveal that
 89 typical discriminators slow down their adaptation to the changes in the new arrival generated data,
 90 and propose a new method to address the challenges. Theoretical studies can make this work more
 91 comprehensive, however, we have not explored it in the paper, since it is beyond the scope of this
 92 paper. Moreover, while the proposed method can effectively improve the training of the CNN-based
 93 GANs models, combining our method with transformer-based ones is left to be investigated.

94 **References**

- 95 [1] Deepfake. <https://en.wikipedia.org/wiki/Deepfake>.
- 96 [2] Yunjey Choi, Youngjung Uh, Jaejun Yoo, and Jung-Woo Ha. Stargan v2: Diverse image
97 synthesis for multiple domains. In *CVPR*, pages 8188–8197, 2020.
- 98 [3] Ian Goodfellow, Jean Pouget-Abadie, Mehdi Mirza, Bing Xu, David Warde-Farley, Sherjil
99 Ozair, Aaron Courville, and Yoshua Bengio. Generative adversarial nets. *NeurIPS*, 27:2672–
100 2680, 2014.
- 101 [4] Liming Jiang, Bo Dai, Wayne Wu, and Chen Change Loy. Deceive d: adaptive pseudo aug-
102 mentation for gan training with limited data. *NeurIPS*, 34:21655–21667, 2021.
- 103 [5] Tero Karras, Timo Aila, Samuli Laine, and Jaakko Lehtinen. Progressive growing of gans for
104 improved quality, stability, and variation. *ICLR*, 2018.
- 105 [6] Tero Karras, Miika Aittala, Janne Hellsten, Samuli Laine, Jaakko Lehtinen, and Timo Aila.
106 Training generative adversarial networks with limited data. *NeurIPS*, 33:12104–12114, 2020.
- 107 [7] Tero Karras, Miika Aittala, Samuli Laine, Erik Härkönen, Janne Hellsten, Jaakko Lehtinen,
108 and Timo Aila. Alias-free generative adversarial networks. *NeurIPS*, 34:852–863, 2021.
- 109 [8] Tero Karras, Samuli Laine, and Timo Aila. A style-based generator architecture for generative
110 adversarial networks. In *CVPR*, pages 4401–4410, 2019.
- 111 [9] Tero Karras, Samuli Laine, Miika Aittala, Janne Hellsten, Jaakko Lehtinen, and Timo Aila.
112 Analyzing and improving the image quality of stylegan. In *CVPR*, pages 8110–8119, 2020.
- 113 [10] Diederik P Kingma and Jimmy Ba. Adam: A method for stochastic optimization. *arXiv*
114 *preprint arXiv:1412.6980*, 2014.
- 115 [11] Cornelius Lanczos. An iteration method for the solution of the eigenvalue problem of linear
116 differential and integral operators. 1950.
- 117 [12] Haozhe Liu, Bing Li, Haoqian Wu, Hanbang Liang, Yawen Huang, Yuexiang Li, Bernard
118 Ghanem, and Yefeng Zheng. Combating mode collapse in gans via manifold entropy estima-
119 tion. *arXiv preprint arXiv:2208.12055*, 2022.
- 120 [13] Haozhe Liu, Wentian Zhang, Bing Li, Haoqian Wu, Nanjun He, Yawen Huang, Yuexiang Li,
121 Bernard Ghanem, and Yefeng Zheng. Adaptivemix: Improving gan training via feature space
122 shrinkage. In *CVPR*, 2023.
- 123 [14] Lars Mescheder, Andreas Geiger, and Sebastian Nowozin. Which training methods for gans
124 do actually converge? In *International conference on machine learning*, pages 3481–3490.
125 PMLR, 2018.
- 126 [15] Adam Paszke, Sam Gross, Soumith Chintala, Gregory Chanan, Edward Yang, Zachary DeVito,
127 Zeming Lin, Alban Desmaison, Luca Antiga, and Adam Lerer. Automatic differentiation in
128 pytorch. 2017.
- 129 [16] Hung-Yu Tseng, Lu Jiang, Ce Liu, Ming-Hsuan Yang, and Weilong Yang. Regularizing gener-
130 ative adversarial networks under limited data. In *CVPR*, pages 7921–7931, 2021.
- 131 [17] Ceyuan Yang, Yujun Shen, Yinghao Xu, Deli Zhao, Bo Dai, and Bolei Zhou. Improving gans
132 with a dynamic discriminator. *NeurIPS*, 2022.
- 133 [18] Ceyuan Yang, Yujun Shen, Yinghao Xu, and Bolei Zhou. Data-efficient instance generation
134 from instance discrimination. *NeurIPS*, 34:9378–9390, 2021.
- 135 [19] Fisher Yu, Ari Seff, Yinda Zhang, Shuran Song, Thomas Funkhouser, and Jianxiong Xiao.
136 Lsun: Construction of a large-scale image dataset using deep learning with humans in the
137 loop. *arXiv preprint arXiv:1506.03365*, 2015.
- 138 [20] Han Zhang, Zizhao Zhang, Augustus Odena, and Honglak Lee. Consistency regularization for
139 generative adversarial networks. *arXiv preprint arXiv:1910.12027*, 2019.